Dry-Jet Wet Electrospinning of Native Cellulose Microfibres with Macroporous Structures from Ionic Liquids

Mohamed Basel Bazbouz[1], Mark Taylor[1], Daniel Baker[2], Michael E. Ries[2], Parikshit Goswami[3]

[1]School of Design, University of Leeds, Leeds, LS2 9JT, United Kingdom.
[2]School of Physics and Astronomy, University of Leeds, Leeds, LS2 9JT, United Kingdom.
[3]Department of Fashion and Textiles, University of Huddersfield, Huddersfield, HD1 3DH, United Kingdom.

ABSTRACT

In this study, we have provided a review of electrospun cellulose micro/nanofibres from ionic liquids and co-solvents from which we identify a lack of previous studies focusing on the structural morphology of the dry-jet wet electrospun native cellulose fibres from ionic liquids. We have therefore aimed to investigate factors influencing the structural morphology of cellulose/ionic liquid electrospun fibres and investigate the coagulation parameters on this morphology. The electrospinning of 10% w/v cellulose/([C2MIM][OAc] /MIM) (1/1, v/v) solution was shown to produce macroporous fibres with average diameters of 2.8±1.4 µm with pore sizes from 100-200 nm. We have found that coagulation bath type and immersion time affect the morphological structure of the electrospun fibres. The fibre spinnability, formation, and morphological structure are mainly dependent on the method used to collect and coagulate/solidify the fibres. The physical properties of the dissolved cellulose were measured and these are discussed in terms of the solution spinnability. The structural morphology of the electrospun cellulose fibres was characterised by SEM, and lastly the extraction of ionic liquid from the fibre body was confirmed by ^{1}H NMR. The electrospun cellulose fibres morphology shows the formation of both micron and nanometre sized fibres with different morphological "macroporous" structures.

INTRODUCTION

Native cellulose, the most abundant natural resource on earth, is a linear polysaccharide and known for its excellent biocompatibility, biodegradability, physical strength, chemical resistance, thermal and mechanical properties and regenerative and sustainable properties[1, 2]. It has been widely used as a high affinity with other substances, in textile, paper and packaging industries, catalyst carriers, insulation clothing and in biomedical material fields[3-6]. The use of native cellulose is traditionally found in wood based paper and cotton based textile fibre industries.

With the ability to regenerate cellulose, a range of modification possibilities with regard to the material macrostructure will be achieved by changing the process parameters during dissolution and coagulation[7-9]. Regenerated cellulose fibres are nowadays being used as the basis of functionalised fibres and reinforced composites fibres[10-11]. Fabrication and regeneration of native cellulose fibres have drawn great attention in recent years[12-17]. However, cellulose regeneration has been long struggling with the use of environmentally hazardous solvents such as N-methylmorpholine-N-oxide (NMMO)[18], N-methylmorpholine N-oxide/water (NMMO/water)[19-21], NaOH/urea aqueous solution[22-23], lithium chloride/dimethylacetamide (LiCl/DMAc)[6, 20, 24, 25] and dimethyl sulfoxide (DMSO)/trimethylamine (TMA)/sulphur dioxide (SO_2)[26]. Moreover, cellulose is seldom soluble in common solvents due to its considerable inter and intra molecular hydrogen bonding. Furthermore, its high crystallinity supported by an intricate hydrogen bonding network and dense packing of polymer sheets by hydrophobic interaction also restrict its solubility in common solvents[27]. Basically, the most common of these solvents so far is the N- methylmorpholine N-oxide (NMMO) which today represents a significant and growing industry for producing textile fibres under the generic name of Lyocell[28]. As a result, it is difficult to create non-derivative cellulose fibrous membranes because it cannot be dissolved in common solvents or melted. Therefore, selecting proper solvents is important in completing the regeneration process of cellulose. A huge amount of effort has been dedicated for several decades to find effective and eco-friendly solvents[29].

"Correspondence to: Mohamed Basel Bazbouz (E-mail: m.b.bazbouz@leeds.ac.uk)."

Ionic liquids (ILs), organic molten salts with low melting points, low or zero vapour pressure, large liquid ranges and high thermal stability, can be used for direct dissolution of cellulose[30-34]. Ionic liquids have been considered as potential green solvents for both polar and nonpolar compounds[35] and have exhibited a large number of chemical, physical, and electrical properties[36-38]. They have been used in regeneration of cellulose into gels, fibres, and films by controlling their chemical composition[39-42]. Regenerated cellulose fibres in the nanometre range display improved properties, such as high surface area to mass ratio, high length to diameter ratio and enhanced surface reactivity[43]. Electrospinning, first patented in 1934[44-48], is one of the simplest and most effective widely used techniques for producing micro/nanofibres from a wide variety of polymers, polymer blends and nanoparticle-impregnated polymers[49-54]. This revolutionary technique is driven by an external electric field on the surface of applied polymeric fluids either in a molten polymer state or in a polymer solution state or even in polymer solutions incorporated with functional particles[55-56].

The nanoscale cellulose fibres have been researched in various applications in technical textiles such as tissue engineering, wound dressing, filtration, fire resistant and antibacterial cellulose fibres[5, 57-60]. However, electrospinning of natural biopolymers such as cellulose is still a challenge and the basic reason for this is due to either the environmentally non-friendly traditional solvents or the rheological complexity of cellulose dissolved in ionic liquids[29]. Although ILs can dissolve cellulose very well, electrospinning of cellulose dissolved in ILs is difficult and hard to control for continuous jets and nanofibre production. In other words, the difficulties of the solidification mechanism by drying of the jet and evaporating of the solvent components and thus the fabrication of cellulose electrospun nanofibre with ILs are because of the high viscosity of ILs, the strong interactions with the cellulose molecules, the rigidity of cellulose chains and the very low vapour pressure property of ionic liquids[36, 59 - 70]. Furthermore, the high viscosity of the polymer solvent and the zero volatility of ILs lead to the standing up of the electrospun fibres vertically, and to the adhesion and contraction of the wet fibres during the electrospinning[6].

Recently, research was published to overcome the challenges of spinnability of cellulose with ionic liquids. Such research used co-solvents with ionic liquids to decrease the viscosity[66, 68] and surface tension[61] of the solvent without any cellulose precipitation, decrease the entanglement density of the network[66], and increase electrical conductivity[17], reactivity and processability of cellulose in the solvent[61, 62, 66-70]. In fact, it has been demonstrated that co-solvents, which act as a precursor for imidazolium-based ionic liquids, are necessary for some reactions to be executed[71]. In addition, researchers used coagulation liquid medium to coagulate the spun fibres for dual goals, the first is to dissolve and wash off the ionic liquid within the coagulant and the second is to control the morphology of the regenerated electrospun fibres[72]. It has been indicated clearly that as far as coagulant liquids are of different polarity (e.g. polarity index from low to high: acetone \ ethanol \ water), the spun fibres and/or film will have different structural properties such as porosity and crystallinity[72-74]. However, Table 1 reviews and summarises all published work, based on the best of the authors' knowledge, of electrospinning of nanofibres from native cellulose dissolved in ionic liquids (ILs)[36, 59-70]. We can perceive from this review a lack of previous studies focusing on the structural morphology of the dry-jet wet electrospun native cellulose fibres from ionic liquids.

In this study, the dry-jet wet electrospinning process of native cellulose in a mixture of room temperature ionic liquid 1-ethyl-3-methylimidazolium acetate [C2MIM][OAc] and co-solvent 1-Methylimidazole (MIM) to produce micro/nanosized cellulose fibres was investigated. We have chosen this ionic liquid [C2MIM][OAc] from the large array of possible ionic liquids, as a result of its desirable properties, such as low toxicity, low viscosity, low melting temperature, low corrosiveness and high cellulose dissolution capacity[75-77]. It has the advantage over most other ILs of being the most efficient and handling solvent at disrupting the intermolecular hydrogen bonding network in cellulose at room temperature[64, 78]. In addition, we have choose the MIM co-solvent which is a precursor for many imidazolium-based ILs in general and for [C2MIM][OAc] in particular. Furthermore, based on its viscometry and solubility data, it increases dramatically the dissolution rate of cellulose and thus provides better solubility of cellulose at lower solution viscosity[79]. We have used our laboratory dry-jet wet-electrospinning setup, which is modified especially for the electrospinning of cellulose with ionic liquids with a coagulation bath containing water or ethanol that act as a co-solvent for the ILs and an anti-solvent for the cellulose, removing the ILs, and coagulating the electrospun fibre. A grounded charge, in the form of flat metallic sheet was covered in halves with aluminium foil and nonwoven fabric and immersed at the bottom of coagulation bath filled with water or ethanol to receive the cellulose fibres. It is

worth noting that the dry-jet wet electrospinning is different from the dry-jet wet spinning[79]. Dry-jet wet spinning technology "also called air-gap wet spinning" which can be used to spin high-performance fibers combines both the advantages of melt spinning through the elongational flow in the air-gap region, and wet spinning through the double diffusion in the coagulation bath[80-84].The dry-jet wet electrospinning provides a simple, fast practical and economically attractive method of fabricating polymer micro/nanofibres[36, 60-71].

The aim of this study is to discover the key factors influencing cellulose/ionic liquid electrospun fibre properties and explore the coagulation parameters which are coagulation type and time on the electrospun cellulose fibre structures. It has been found in our studies that the fibre spinnability, formation, structure and morphology are mainly determined by the method used to collect and solidify the fibres. The viscosity, surface tension and electrical conductivity of the dissolved cellulose in [C2MIM][OAc]/MIM were measured and discussed. The structural morphology of the electrospun cellulose fibres was characterised and assessed by SEM and ^{1}H NMR. We aim through this study to give a fundamental understanding of the electrospinning of cellulose and to improve the properties and the performance of the cellulose nanofibres produced by electrospinning.

Table I

MATERIALS AND METHODS

Materials

Microcrystalline cellulose powder (Avicel® PH-101) (Mw = 53470, Mn = 24235) with specific weight of 0.600 g.cm^{-3}, ionic liquid 1-Ethyl-3-methylimidazolium acetate [C2MIM][OAc] with molecular weight of 170.21 g/mol and specific weight of 1.027 g.cm^{-3} at 25 ℃, co-solvent 1-methylimidazole (MIM) with molecular weight of 82.10 g/mol, specific weight of 1.03 g.cm^{-3} at 25 ℃ and boiling point of 198 ℃, distilled water, ethanol with specific weight of 0.7893 g.cm^{-3}, heavy water (deuterium oxide) (D2O) and liquid nitrogen were purchased from Sigma- Aldrich (Gillingham, UK) and were used without further purification.

Solution preparation and electrospinning

Cellulose samples were dried at 70 ℃ for 3 h in a vacuum oven. Then predetermined weight of dried cellulose was dispersed in appropriate volume of co-solvent (MIM) and was allowed to stay for 10 min in a sealed vessel. Subsequently, the same volume of ionic liquid [C2MIM][OAc] was added and the vessel content was then mechanically stirred using a magnetic stir bar in a temperature controlled oil bath at 70 °C for 12 h. Cellulose was dissolved in ([C2MIM][OAc]/MIM) (1/1, v/v) at concentrations of 0, 1, 6, 7, 8, 9, 10, 12, 15% (w/v). A dry-jet wet electrospinning technique was employed to produce micron-nano scale cellulose flexible fibres. Each cellulose solution concentration was fed from a 5 mL capacity syringe (Fisher Co., Leicestershire, UK) to a vertically orientated (19 gauge) blunt-ended metal needle 'spinneret' via Teflon tubing. The inner and outer diameter of the needle were 0.686±0.038 mm and 1.067±0.013 mm, respectively. The volume feed rate was digitally controlled by a positive displacement microprocessor syringe pump (Model 200 Series, Kd Scientific Inc., USA). The needle was connected to one electrode of a high voltage direct-current power supply, which is capable of generating a voltage up to 60 KV (EH60P1.5, Glassman, USA). A flat metallic sheet of (20, 5, 2) mm dimensions was covered in halves with aluminium foil and meltspun polypropylene (PP) nonwoven fabric with fineness of 3±0.30 (Denier per fibre) and grounded as the counter electrode on the bottom of a coagulation bath filled with ethanol to receive and precipitate the cellulose fibres. We have chosen this collector covering system for comparison between the precipitated cellulose and meltspun polypropylene fibre diameters.
Typical operating electrospinning process parameters were flow rates of 0.15 mL/h, applied voltage of 20 kV, and a vertical electrospinning working distance between the tip of the needle and the surface of the ethanol bath of 12 cm. The experiments were maintained under environmental conditions at room temperature of 23±2 °C and 25-30% RH relative humidity. When the electrospinning was completed, the entangled web of flexible fibres was removed. In order to study the effect of the coagulation bath system on the structural morphology of the electrospun cellulose fibres, four main exposure and immersion systems were employed. In practice,

the first is to expose the collected 10% (w/v) cellulose fibres from ethanol coagulation bath after electrospinning to liquid nitrogen. The second is to put the collected 10% (w/v) cellulose fibres into an oven at 70 ℃ for 24 h. The third is to immerse the collected 10% (w/v) cellulose fibres into ethanol bath at room temperature for 1, 3 and 5 days. The fourth is to immerse the collected 10% (w/v) cellulose fibres into distilled water bath at room temperature for 1, 3 and 5 days.

Characterisation

Samples nomenclature were coded in this work as 'CX%' which identify the electrospinning cellulose solutions at different concentrations. 'X' indicates the concentration of cellulose % (weight/volume) (w/v) in a binary of [C2MIM][OAc]/MIM (1:1). The 2D surface morphology of the electrospun cellulose fibres were observed by scanning electron microscopy (SEM; Hitachi S-2600N, Japan) with a secondary electron detector. All the air dried samples were cut into small sizes, adhered to an aluminium stub 12.7 mm diameter with the aid of carbon adhesive tapes and sputter coated with high resolution sputter coater (Emitech K550X, UK) with gold layers under high vacuum. An acceleration voltage of 3 - 5 kV was used with a typical working distance of 5.9-10.9 mm. The fibre diameters in each sample were evaluated from different regions of the sample stub. Images were captured at different magnifications in the range of 500x to 30000x for all electrospun cellulose fibres. The average fibre diameters from SEM images were measured by means of image analysis (SemAfore 5.21 software, JEOL CO., Finland). The pore size of the macropores on the fibres were measured with at least 50 measurements to determine the mean size.

The viscosities of all prepared cellulose/([C2MIM][OAc]/MIM) solutions at different concentrations were measured on a Brookfield digital viscometer (Brookfield DV-II Viscometer, USA). Readings were taken at 23±2 °C using spindles and chamber of SC4-34/13R and SC4-25/13R. Polymer solution volume of 9.4 mL for C0, C1 and C6% (w/v) and polymer solution volume of 16.1 mL for C7 to C15% (w/v) samples were placed in a beaker, into which the spindle of the viscometer was immersed and rotated at a shear rate in the range from 60 to 1 rpm (equivalent to 1 – 0.017 sec^{-1}), in order to characterise the rheological properties of the cellulose/([C2MIM][OAc]/MIM) solutions. Each sample was allowed to equilibrate at the measurement temperature for 10 min before the shear rate was increased.

The surface tension of [C2MIM][OAc], MIM and solutions of cellulose/([C2MIM][OAc]/MIM) was measured and analysed by means of the pendant drop method using a CAM 200 contact angle goniometer (KSV Instruments Ltd., Finland). A pendant drop method in six parallel measurements using a micro-syringe with an automatic dispenser and a CCD fire wire camera (512x480) with telecentric zoom optics combined with LED based background lighting allowing capturing images at frame intervals from 10 ms to 1000s was carefully conducted. The surface tension S_T was calculated by using the equation;

$$S_T = \frac{g.\rho.d_e^2}{S_f} \quad [1]$$

Where g is the acceleration of gravity, ρ is the difference in density of the air and the polymer solution, d_e is the equatorial diameter of the droplet and S_f is the shape factor, as referenced in [85]. Polymer solution densities were measured by recording the mass of 1 ml of the polymer solutions in volumetric flasks at 23±2 °C and were used in surface tension measurements. Each measurement was replicated three times and the mean values were used in surface tension measurements.

Electrical conductivity of all cellulose/([C2MIM][OAc]/MIM) solutions at different concentrations was examined by Novocontrol broadband dielectric impedance spectrometer (Montabaur, Germany), with integrated alpha-A high performance frequency analyser in 0.1 Hz to 10 MHz frequency range. Samples were tightened by using vacuum sealed parallel electrodes (diameter of 18 mm) as a specimen holder cell with a spring for sealing out the air and the data was analysed by using WinFit software. All measurements were carried out at a temperature of 23±2 °C and the spectrometer was set to a bias of 1 volt and each sample was measured between frequency sweeps of 1.0 Hz to 1.8 MHz.

For the ^{1}H NMR analysis, ^{1}H spectra were recorded at 23±2 °C using a wide-bore Bruker Avance II spectrometer (Bruker BioSpin AG, Switzerland) with a proton resonant frequency of 400 MHz. Spectra were obtained using a single 90° pulse sequence with a pulse length of 6.5 µs, acquisition time of 1.25 s and a delay time of 3 s. The cellulose fibres were then suspended in 1.5 ml of D2O with high isotopic purity and transferred to a 5 mm NMR tube for measurement after 5 days of D_2O immersion.

RESULTS AND DISCUSSION

Viscosity, surface tension and electrical conductivity of cellulose/([C2MIM][OAc]/MIM) solutions

The shear viscosities of dissolved cellulose in a binary of [C2MIM][OAc]/MIM (1:1 by volume) at cellulose concentration of 0, 1, 6, 7, 8, 9, 10, 12, and 15% (w/v) were plotted under room temperature of 23±2 °C as a function of shear rate and shown in figure 1. The shear viscosities of the dissolved cellulose increased noticeably with the increase in cellulose concentration which are to be expected for all types of polymer solutions. Generally, as the viscosity of the dissolved cellulose increased, the chain overlap/entanglement of the cellulose molecules will also be increased, to a sufficient level to cause the elongation of the jet and to prevent breakup of the ejected jet, but not high enough to suppress capillary instability to happen, resulting in great difficulty in electrospinning and formation of beads in the nanofibrous web morphology. All the curves showed shear thinning behaviour, i.e., the viscosity decreases as the shear rate increases. That indicates that all the dissolved cellulose in a binary [C2MIM][OAc]/MIM are non-Newtonian liquids[68].

Figure 2 (A) shows the dependence of shear viscosity of a binary [C2MIM][OAc]/MIM solvent mixture on cellulose concentration C (% w/v) at different shear rate (γ=0.0167 to γ=1 [sec^{-1}]). The curves showed three different regimes which are the dilute regime, semidilute unentangled regime, and semidilute entangled regime. The dependence of viscosity η at shear rate of 0.1 - 1.sec^{-1} of a binary [C2MIM][OAc]/MIM solvent mixture on cellulose concentration is shown in figure 2 (B) which has been obtained from figure 2 (A). The critical concentrations and the values of the slopes are determined using the cross model[86]. Based on figure 2 (B), the increase of the viscosity η can be identified with a power law dependence for each concentration C regime in equation 2[87].

$$\eta = k.C^{n} \qquad [2]$$

Figure 1

In the dilute regime with low cellulose concentrations, the shear viscosity increases linearly with increasing concentration with an exponent n= 1 and the interaction between discrete cellulose chains is low. Above a critical polymer concentration C=6%, the polymer chains can interact without entanglement (unentangled semidilute regime, with an exponent (n = 3.9)). While, in the semidilute entangled regime (C=10% w/v and above), the shear viscosity follows a scaling mode of concentration with an exponent n of 3.5 and favours chains entanglement and thus stronger interactions. In fact, this is consistent with that observed for the cellulose acetate in alcohols/DMSO[88] and celluloses in an ionic liquid [AMIM][Cl][89]. For cellulose (Avicel® PH-101) (Mw = 53470), the boundary concentrations were found at C=6 and C=10 (% w/v) in a binary [C2MIM][OAc]/MIM solvent mixture. We have found that the electrospun fibres morphology depend strongly on the spinning dope viscosity and its molecular interaction as shown in figure 5. Finally, for cellulose (Avicel® PH-101) with a binary [C2MIM][OAc]/MIM (1/1) solvent mixture, continuous flexible fibres can only be electrospun for cellulose concentrations of 10% w/v and above. In comparison, individual porous grains (monoliths) or blocks are observed for cellulose concentrations lower than C= 10% w/v.

Figure 2

The surface tension of dissolved cellulose in a binary mixture of [C2MIM][OAc]/MIM (1:1 by volume) at cellulose concentration of 6, 7, 8, 9, 10, 12, and 15% (w/v) and the surface tension of pure [C2MIM][OAc] and co-solvent MIM are given in table 2. Each sample was measured, analysed and calculated in triplicate and the mean values of the triplicates and the standard deviation were calculated and recorded. The surface tension values of the dissolved cellulose in [C2MIM][OAc]/MIM decreased with increase in cellulose concentration.

For example the surface tension decreased from 41.82±1.12 $mN.m^{-1}$ for [C2MIM][OAc]/MIM (1/1: v/v) and 40.48±0.32 $mN.m^{-1}$ for C 6% w/v to 37.19±0.91 $mN.m^{-1}$ for C 15% w/v. In addition, our reported surface tension values of the pure solvents used are as follows, the surface tension of ionic liquid [C2MIM][OAc] at room temperature is 45.78± 0.76$mN.m^{-1}$, and the surface tension of co-solvent MIM at room temperature is 34.3± 0.55 $mN.m^{-1}$. The standard deviation values are low which indicate that the values tend to be close to the mean (the expected value). It has been indicated that cellulose performs as a polymeric surfactant when dissolved in [C2MIM][OAc], and in general most polymers perform as surfactants when dissolved in a solvent[90-92]. It is generally considered that the surface tension plays an important role in determining the range of polymer solution concentrations from which continuous uniform nanofibres can be obtained in electrospinning[93]. This is consistent with most properly chosen electrospun polymer solutions (whatever the method of electrospinning) where the viscoelastic forces completely dominate the surface tension. In other words, a direct correlation has been observed between uniform fibre diameter and polymer solution viscosity and surface tension[94]. In comparison, when low molecular weight polymers are used or polymer solution concentration is significantly reduced, the viscoelastic forces dramatically diminish and thereby the surface tension plays a strong role in the morphology of the resulting fibres[95]. Hence, when the surface tension forces are dominant, they attempt to reduce surface area per unit mass, and thus beaded fibres are consequently produced[96]. Briefly, it is clearly seen that the concentration of cellulose and the co-solvent MIM in [C2MIM][OAc] strongly affected the surface tension of solution. In other words, the surface tension can be reduced by increasing the concentration of cellulose and the co-solvent MIM in [C2MIM][OAc].

Table II

The electrical conductivity σ as a function of frequency [Hz] of dissolved cellulose in a binary of [C2MIM][OAc]/MIM (1:1 v/v) solutions at cellulose concentration of 6, 7, 8, 9, 10, 12, and 15% (w/v) is presented in the figure 3. The value of the electrical conductivity at the lowest measured nearly zero frequency has been considered as a direct current (DC) conductivity for comparative purpose which suits the case of the DC high voltage power supply used in our work. However, figure 3 shows all electrical conductivity curves are increasing as the frequency increased. Therefore, differences between all dissolved cellulose solutions were assessed at the lowest frequency (1.0 Hz, nearly zero). For the dissolved cellulose at various concentration systems, the electrical conductivity increases as the cellulose concentration decreased. For example, the electrical conductivity increases from 263$\mu S.cm^{-1}$ at 15% (w/v) cellulose concentration to 413 $\mu S.cm^{-1}$ at 6% (w/v) cellulose concentration. In other word, these curves indicate that with increasing [C2MIM][OAc]/MIM content, the charge density of the cellulose solution increased. In fact, this is expected as [C2MIM][OAc] ionic liquid exhibits a high electric conductivity at ambient temperature of 2500 $\mu S.cm^{-1}$ [97], and pure cellulose is a material which is electrically insulating with electrical resistivity of 10^{12} $\mu\Omega.cm$ and thus its electrical conductivity is 10^{-12} $\mu S.cm^{-1}$ [98]. As a matter of fact, the electrical conductivity of the polymer solution mirrors the charges density on the jet and thus higher elongation forces are imposed to the fibres under an applied electrical field. In other words, under the same applied voltage and spinning distance, a polymer solution with higher electrical conductivity will cause higher elongation to the jet along its length and thus electrospinning fibres with smaller diameter [99]. Briefly, the electrical conductivity of the polymer solution is a key factor in determining the electrospinning current, net charges density, fibres morphology and electrospinning ease[95].

Electrospinning of cellulose/([C2MIM][OAc]/MIM) solutions

The cellulose/([C2MIM][OAc]/MIM) (1/1, v/v) solutions were electrospun at different concentrations of 6, 7, 8, 9, 10, 12, 15% (w/v) by using a modified dry-jet wet electrospinning technique. In this study, ionic liquid [C2MIM][OAc], having lower viscosity, higher conductivity, higher solubility in water and higher suitability for cellulose dissolution than other ionic liquids used in electrospinning of cellulose such as [C4MIM][Cl] and [AMIM][Cl], was utilized as a solvent for cellulose[60, 63, 65-69]. These enhanced properties have given us ease of electrospinning process and allowed us to achieve smaller fibre diameters. In addition, we have chosen the co-solvent MIM as it has been confirmed that it provides better solubility of cellulose with increased dissolution rate and lower solution viscosity among the other co-solvents such as DMSO and DMAc used in the dry-jet wet spinning of cellulose[79]. In this technique, the metal needle ‘spinneret’ connected to a Teflon tube and containing the cellulose/([C2MIM][OAc]/MIM) solution was placed vertically to the ethanol

coagulation bath. In order to solidify the electrospun fibres, a dry-jet wet electrospinning was used with a coagulation bath containing water or ethanol. When water was used as a coagulation bath, it was observed that all cellulose fibres landed at the surface of the water bath, piled up and did not sink through the water. As a result, the wet cellulose fibres ([C2MIM][OAc] is a non-volatile solvent) merge with each other like a film without forming fibrillation as shown in figure 4. This could be supported by the fact that the specific weight of water is higher than the measured specific weight of cellulose (Avicel)/([C2MIM][OAc]/MIM) solutions at all studied concentrations. Hence, the specific weight of [C2MIM][OAc], MIM, and cellulose (Avicel) are 1.027 $g.cm^{-3}$, 1.03 $g.cm^{-3}$ and 0.6 $g.cm^{-3}$ respectively. However, to electrospin cellulose ([C2MIM][OAc]/MIM) fibrous assembly based on dry-jet wet electrospinning, a coagulation bath containing ethanol is suitable as ethanol has a specific weight of 0.7893 g/cm^3 and the measured specific weight of cellulose solutions are in range of 1.035 $g.cm^{-3}$ for 6% (w/v) and 0.993 $g.cm^{-3}$ for 15% (w/v) cellulose concentration.

Figure 3

Figure 4

It is well known that the dry-jet wet electrospun cellulose fibre diameter and morphology is mainly controlled by changing the cellulose concentration, the electrospinning process parameters, the feeding rate of fibres and the extraction rate of ionic liquid and co-solvent[36, 60-71]. We have found that the cellulose concentration played a major role in cellulose fibre diameter, whereas the processing parameters such as the applied voltage and electrospinning working distance have little impact on the cellulose fibre diameter. The total flow rate of the cellulose solution for stable electrospinning was considered based on the strength of the applied electric field which will control the mass gravity, and the syringe pump flow rate. Because [C2MIM][OAc] is a non-volatile solvent and the boiling point of MIM is 198 ℃, complete extraction of the [C2MIM][OAc] (washing of the [C2MIM][OAc]) during electrospinning process and ethanol coagulation bath was not possible. Strictly speaking, in order to investigate the effect of the ethanol coagulation bath on the extraction rate of [C2MIM][OAc] and thus the structural morphology of the electrospun cellulose fibres, we have employed four main exposure and immersion systems. The first system is to expose the collected cellulose fibres from the ethanol coagulation bath after electrospinning to a liquid nitrogen. Liquid Nitrogen will freeze and solidify the electrospun fibres rapidly allowing us to examine the structural morphology of the cellulose fibres and to assess the extraction rate directly after removal from the ethanol bath. The same is true for oven exposure as far as the residue of the co-solvent MIM will be completely evaporated. It has been already reported by Miyauchi et al. that ionic liquid [C2MIM][OAc] has high solubility in ethanol[63]. Nevertheless, based on the literature works, the extraction rate of ionic liquid from electrospun cellulose fibre during immersion in the ethanol coagulation bath was not clear. Furthermore, the effect of immersing the cellulose fibre in ethanol or water and the extraction rate of ionic liquid on the structural morphology of the electrospun cellulose fibres was not presented, to the best of the author's knowledge, in published literature[36, 59-70]. Based on the presented exposure and immersion systems, we will show hereinafter by the SEM images the structural morphology of the electrospun micro/nanosized cellulose fibres.

Morphology of dry-jet wet electrospun cellulose fibres

Figure 5 (A-F) shows the SEM images of the cellulose fibres that were electrospun from the ([C2MIM][OAc]/MIM) solutions at 6, 8, 9, 10, 12, 15% (w/v) cellulose concentration and directly immersed into distilled water bath at room temperature for 5 days after collection from ethanol coagulation bath. At the cellulose concentration of 6, 8, 9% (w/v), as shown in figure 5 (A-C), many intensified and connected grains (monoliths) or blocks with rough surfaces and porous structures were found. In fact, this is in full agreement with the unentangled semidilute regime in the dependence of viscosity η at shear rate of 0.1 [sec^{-1}] curve presented above in figure 2 (B). As explained above, in the unentangled semidilute regime, the polymer chains can interact without entanglement which will prevent the continuous fibre formation. As the concentration of cellulose increased to 10, 12, and 15% (w/v), continuous cellulose fibres with rough surfaces and porous structures were achieved. This is also consistent with the curve in figure 2 (B) that continuous flexible fibres can only be electrospun for (Avicel) cellulose concentrations of 10% w/v and above.

The average diameters of these electrospun fibres were non-uniform in fibre diameters and were in averaged micron sizes of 2.8±1.4 µm, 6.25±1.25 µm and 7.75±1.75 µm for 10, 12, and 15% (w/v), respectively. When the cellulose solution concentration of 15% w/v was electrospun, fibres with greater diameter were obtained. This is attributed to the larger content of cellulose that would increase the viscosity and thus obstruct the whipping motion during electrospinning process. Generally, the high viscosity, low electrical conductivity and non-volatility of the [C2MIM][OAc] limited the electrospun fibres to be just in micron-sized diameters. One interesting observation is the precipitated electrospun cellulose fibres on meltspun polypropylene (PP) fibres with fineness of 3±0.30 (Denier per fibre) in figure 5 (D, E) for comparison between dry-jet wet electrospun and melt spun fibres diameters. In addition, it is worth noting that the diameters of dry-jet wet spun cellulose fibres were ranged from 109.17 - 202.86 Titer Denier (dtex) after drawing with a draw ratio of 5 – 10 [100].

To further support this hypothesis related to the porous structures of these fibres after immersion into distilled water for 5 days, we presented SEM images for electrospun cellulose fibres after collection from ethanol coagulation bath and exposed to different exposure systems. Figure 6 (A, B) shows the SEM images of the collected cellulose fibres at 10% w/v concentration from the ethanol coagulation bath after electrospinning course and directly being exposed to liquid nitrogen (A) or put into an oven at 70 ℃ for 24 h (B). The morphologies of electrospun cellulose fibres after liquid nitrogen exposure were mainly smooth with some bulges on the surface of the fibres. The bulges phenomenon can be explained by the skin formation during electrospinning process by the action of ethanol coagulation bath[67]. Nevertheless, although almost all of the cellulose/[C2MIM][OAc] was preserved inside the fibres, part of [C2MIM][OAc] simultaneously tried to go out of the cellulose fibre into ethanol to form some bulges.

Figure 5

The SEM image in figure 6 (B) indicated that [C2MIM][OAc] was kept inside the cellulose fibre body during the electrospinning course and ethanol bath collection due to its non-volatility. Hence, part of the co-solvent MIM has evaporated during the electrospinning and any residues were completely evaporated after drying at an oven at 70 ℃ for 24 h. It can be confirmed clearly that due to [C2MIM][OAc] is a non-volatile solvent, complete removal of the [C2MIM][OAc] during the electrospinning course was not achieved.

Figure 6

Figure 7 (A-C) shows the SEM images of the collected cellulose fibres at 10% w/v concentration from the ethanol coagulation bath after electrospinning and directly being immersed in ethanol bath at room temperature for 1, 3 and 5 days. As expected, the bulges on the surface of the cellulose fibres were denser and larger with increasing immersion time in ethanol bath. It is known that ethanol and water can completely dissolve [C2MIM][OAc] used in the dissolution of cellulose and that supports the hypothesis of [C2MIM][OAc]/ethanol exchange which was not completed by immersion with ethanol bath[63]. In other words, five days were not sufficient to extract the ionic liquid [C2MIM][OAc] from the cellulose fibre body. In contrast, when immersing collected cellulose fibres at 10% w/v concentration from the ethanol coagulation bath after electrospinning in distilled water for 5 days, electrospun fibres with macroporous structure with pore sizes from 100–200 nm were obtained indicating better extraction of [C2MIM][OAc] ionic liquid from the fibre body.

Figure 7

Figure 8

Figure 8 (A-C) shows the SEM images of the collected cellulose fibres at 10% w/v concentration from the ethanol and directly were immersed in distilled water bath at room temperature for 1, 3 and 5 days. After one day of immersion, cracks and bulges appeared on the surface of the cellulose fibres as shown in figure 8 (A). On the third day, as shown in figure 8 (B), the cracks and bulges became larger and more numerous, indicating that water dissolves [C2MIM][OAc] faster than ethanol. Figure 8 (C) shows that [C2MIM][OAc] was almost completely dissolved in the water and the fibre surfaces have become rough and porous due to the removal of [C2MIM][OAc].

It is clear from the SEM image in figure 9 that, as water gets in the electrospun fibres to dissolve the ionic liquid [C2MIM][OAc], it leaves nano and macropores along all the surfaces of the fibres. As mentioned before, the macroporous structure "big pores with thin walls" of the fibres is due to the [C2MIM][OAc] traces being removed. One interesting observation that can be made here is that, the pores appear to be uniformly distributed through the length of the fibre. Interestingly, these regenerated macroporous electrospun cellulose fibres have higher surface area, compared with pure cellulose fibres, which are in great demand for a wide range of applications such as ion-exchange resins, ultra-filtration materials and carriers for catalysts and reagents[101].

Figure 9

Proton nuclear magnetic resonance (^{1}H NMR) characterisation

To further support this observation, removal of the residual [C2MIM][OAc] in the cellulose fibres was confirmed by pulsed ^{1}H NMR. ^{1}H NMR analysis after cellulose fibres immersion in D_2O for the first case, i.e. immediately after immersion, showed the same ^{1}H NMR spectrum of pure D_2O with chemical shift at a range of 4 - 6 ppm, with no detectable presence of the ionic liquid. Figure 10 (B) shows the ^{1}H NMR spectrum of (D_2O) with one OH proton peak at a chemical shift of approximately 4.8 ppm which corresponds to the residual H_2O in D_2O[102, 103]. In contrast, the ^{1}H NMR spectrum of cellulose fibres immersed in D_2O for 5 days presented in Fig. 10(A) shows chemical shifts at 1.34, 1.77, 3.76 and 7.32 ppm. Hence, assignments of the spectral bands, which are labelled a-g, are made with reference to the chemical structure of [C2MIM][OAc] shown in figure 10 (C), presented from our previous work[104]. Due to the effect of ^{1}H-^{1}H dipolar broadening the cellulose spectral bands are not observed in the NMR spectrum. The aforementioned chemical shifts are associated with the [C2MIM][OAc] ionic liquid dissolved in the D_2O[105]. Therefore, this confirms the presence of [C2MIM][OAc] ionic liquid in the water within the five days, which must have been removed from the fibre during that period.

Figure 10

CONCLUSION

In this work, the dry-jet wet electrospinning of cellulose in mixed solvent systems of [C2MIM][OAc]/MIM was researched for the first time. In addition, we have presented a comprehensive review of electrospun cellulose fibres from different types of ionic liquids and co-solvents and their electrospinning conditions and characterisations. The rheological properties of the cellulose/([C2MIM][OAc]/MIM) solutions obtained as a function of concentration of cellulose enabled us to determine the semidilute unentangled and entangled regimes and thus the proper cellulose concentration for electrospinning of continuous fibres. Electrospun cellulose jets collected in a water coagulation bath was film-like without forming fibrillation. In contrast, electrospun cellulose jets collected in ethanol coagulation bath were dive into ethanol forming fibre webs. It has been found that the cellulose (Avicel)/([C2MIM][OAc]/MIM) (1/1, v/v) solutions could only electrospin fibres at a cellulose concentration of 10% w/v (the optimal concentration) and above. It has been also confirmed by exposing the electrospun cellulose fibres into liquid nitrogen and oven temperature that the [C2MIM][OAc], was not completely extracted during the electrospinning course. The use of RTILs and co-solvent ([C2MIM][OAc] and MIM) to electrospin fibres, followed by [C2MIM][OAc] extraction through water immersion, demonstrates an advantage for fibre spinning with macroporous structure. The size of the electrospun cellulose fibres were influenced by the concentration of cellulose in [C2MIM][OAc]/MIM which directly affected the viscosity of cellulose solutions. SEM images showed the formation of both micron and nanometre sized fibres with different morphological structures. ^{1}H NMR provided evidence for the presence of [C2MIM][OAc] ionic liquid within the electrospun fibre. Finally, dry-jet wet electrospinning offers promise in the preparation of micro/nanosized macroporous cellulose fibres for use in a wide range of applications due to the larger surface area.

ACKNOWLEDGEMENT

The authors wish to thank the University of Leeds for financial support. Dr. Emily James in school of chemical and process engineering is gratefully acknowledged for technical assistance with the surface tension measurements. Dr M E Ries is a Royal Society Industry Fellow.

REFERENCES

1. Mannhalter, C. *Sens. & Actuate. B Chem.* **1993**, *11*, 273-279.
2. Klemm, D., Heublein. B., Fink H. P. and Bohn, A. *Angew. Chemie. Int. Ed.* **2005**, *44*, 3358-3393.
3. Son, W.K., Youk, J. H., Lee, T. S. and Park, W. H. *J. Polym. Sci: B Polym. Phys.* **2004**, *42*, 5-11.
4. Nishio, Y. *Adv. Polym. Sci*. **2006**, *205*, 97-151.
5. Nge, T. T. and Sugiyama, J. J. J. Biomed. *Mater. Res: A*. **2007**, *81*, 124-134.
6. Frenot, A., Henriksson, M. W. and Walkenstro, M. P. *J. Appl. Polym. Sci*. **2007**, *103*, 1473-1482.
7. Frenot, A. In Regenerated cellulose fibres; C. Woodings, Ed.; Woodhead Publishing Limited: Cambridge, **2000**, Chapter 3, pp 50-56.
8. Boerstoel, H., Maatman, H., Westerink, J. B. and Koenders BM. *Polymer* **2001**, *42*, 7371-7379.
9. Kotek, R. In Handbook of fibre chemistry; Lewin, M. Ed.; Taylor & Francis, New York, **2006**, Chapter 10, pp 668-764.
10. Nishino, T. In Green composites: polymer composites and the environment; C. Baillie, Ed.; Woodhead Publication Limited, Cambridge, **2004**, Chapter 4, pp 68-74.
11. Tajima, K.; Fujiwara, M.; Takai, M.; Hayashi, J. In Cellulose and cellulose derivatives: Physico-chemical aspects and industrial applications; Kennedy, J. F.; Phillips, G. O.; Williams, P. A.; Piculell, L. Eds.; Woodhead Publishing Limited: Cambridge, **2009**, Part 1(2), pp 9-14.
12. Zhu, S., Wu, Y., Chen, Q., Yu, Z., Wang, C., Jin, S., Ding, Y. and Wuc, G. *Green Chem*. **2006**, *8*, 325-327.
13. Erdmenger, T., Haensch, C., Hoogenboom, R. and Schubert, U. S. *Macromol. Biosci.* **2007**, *7*, 440-445.
14. Feng, L. and Chen, Z. L. *J. Molecule. Liquids*. **2008**, *142*, 1-5.
15. Frey, M. W. *Polym. Rev.* **2008**, *48*, 378-391.
16. Meli, L., Miao, J., Dordick, J. S. and Linhardt, R. J. *Green Chem*. **2010**, *12*, 1883-1892.
17. Isik. M., Sardon, H. and Mecerreyes, D. *Int. J. Molecule. Sci.* **2014**, *15*, 11922-11940.
18. Rosenau, T., Potthast, A., Adorjan, I., Hofinger, A., Sixta, H. Firgo, H. and Kosma, P. *Cellulose*, **2002**, *9*, 283-291.
19. Kulpinski, P. *J. Appl. Polym. Sci.* **2005**, *98*, 1855- 1859.
20. Kim, C. W., Kim, D. S., Kang, S. Y., Marquez, M. and Joo, Y. L. *Polymer*, **2006**, *47*, 5097-5107.
21. Han, S.O., Son, W. K., Youk, J. H. and Park, W. H. *J. Appl. Polym. Sci.* **2008**, *107*, 1954-1959.
22. Cai, J. and Zhang, L. N., *Macromole. Biosci.* **2005**, *5*, 539-548.
23. Qi, H., Sui, X., Yuan, J., Wei, Y. and Zhang, L. *Mater. Eng*. **2010**, *295*, 695-700.
24. McCormick, C. L., Callais, P. A. Jr. and Hutchinson, B. H. *Macromolecules*, **1985**, *18*, 2394-2401.
25. Kim, C. W., Frey, M. W., Marquez, M. and Joo, Y. L. *J. Polym. Sci. B, Polym. Phys.* **2005**, *43*, 1673-1683.
26. Isogai, A., Ishizu, A. and Nakano, J. *J. Appl. Polym. Sci.* **1986**, *33*, 1283-1290.
27. Olsson, C. and Westman, G. *J. Appl. Polym. Sci*. **2013**, *127*, 4542-2548.
28. Krassig, H., Schurz, J., Robert, G., Schliefer, S. K., Albrecht, W., Mohring, M. and Schlosser, H. *Indust. Chem.* **2002**, *7*, 279-332.
29. Swatloski, R. P., Spear, S. K., Holbrey, J. D. and Rogers, R. D. *J. Amer. Chem. Soc.* **2002**, *124*, 4974-4975.
30. Zhang, H., Wu, J., Zhang, J. and He, J. *Macromolecules*, **2005**, *38*, 8272-8277.
31. Heinze, T., Schwikal, K. and Barthel, S. *Macromol. Biosci.* **2005**, *5*, 520-525.
32. Liying, G. In Ionic liquids: applications and perspectives; Kokorin, A. Ed.; InTech, Croatia, **2011**, part 2, Chapter 3, pp 47-60.
33. Wang, H., Gurau, G. and Rogers, R. D. *Chem. Soc. Rev.* **2012**, *41*,1519-1537.
34. Gericke. M., Fardim. P. and Heinze, T. *Molecules*, **2012**, 17, 7458-7502.
35. Sheldon, R. *Chem. Comm.* **2001**, *23*, 2399-2407.
36. Viswanathan, G., Murugesan, S., Pushparaj, V., Nalamasu, O., Ajayan, P. M. and Linhardt, R. J. *Biomacromolecules*, **2006**, 7, 415-418.
37. Buzzeo, M. C., Hardacre, C. and Compton, R. G. *Analy. Chem.* **2004**, 76, 4583-4588.

38. Welton, T. *Chem. Rev.* **1999**, *99*, 2071-2083.
39. Cao, Y., Li, H., Zhang, Y. and He, J. *J. Appl. Polym. Sci.* **2010**, *116*, 547-554.
40. Hermanutz, F., Garr, F., Uerdingen, E., Meister, F., Kosan, B., *Macromol. Symp.* **2008**, *262*, 23-27.
41. Kadokawa, J. I., Murakami, M. A. and Kaneko, Y. A. *Carbohyd. Res.* **2008**, *343*, 769-772.
42. Liu, Z., Wang, H., Li, Z., Lu, X., Zhang, X., Zhang, S. and Zhou, K. *Mater. Chem & Phys.* **2011**, *128*, 220-227.
43. Vasita, R. and Katti, D. S. *Int. J. Nanomed*. **2006**, 1, 15-30.
44. Formhals, A. (Process and apparatus for preparing artificial threads). U.S. Patent 1,975,504, October 2, 1934.
45. Formhals, A. (Method and apparatus for spinning). U.S. Patent 2,160,962, June 6, 1939.
46. Formhals, A. (Artificial thread and method of producing same). U.S. Patent 2,187,306, January 16, 1940.
47. Formhals, A. (Producing of artificial fibres from fibre forming liquids). U.S. Patent 2,323,025, June 29, 1943.
48. Formhals, A. (Method and apparatus for spinning). U.S. Patent 2,349,950, May 30, 1944.
49. Huang, Z. M., Zhang, Y. Z., Kotaki, M. and Ramakrishna S, *Comp. Sci. Tech.* **2003**, *63*, 2224-2253.
50. Persano, L., Camposeo, A., Tekmen, C. and Pisignano, D. *Macromol. Mater. & Eng.* **2013**, *298*, 504-520.
51. Feng, L., Xie, N. and Zhong, J. *Materials*, **2014**, *7*, 3919-3945.
52. Mishra, R., Militkya, J., Bahetia, V., Huanga, J., Kalea, B., Venkataramana, M., Belea, V., Arumugama, G. and Wang, Y. *Text. Pro*. **2014**, *46*, 133-226.
53. Bazbouz, M. B. and Stylios, G. K. *J. Appl. Polym. Sci.* **2008**, *107*, 3023-3032.
54. Bazbouz, M. B. and Stylios, G. K. *Eur. Polym. J.* **2008**, 44, 1-12.
55. Li. D. and Xia, Y. *Adv. Mater.* **2004**, *16*, 1151-1170.
56. Bazbouz, M. B. and Stylios, G. K. *J. Appl. Polym Sci.* **2012**, *121*, 195-201.
57. Nishio, Y. *Adv. Polym. Sci.* **2006**, *205*, 97-151.
58. Cuculo, F. A., Aminuddin, N. and Frey, M. W. In Solvent spun cellulose fibres, D. R. Salem Ed.; Hanser Gardner Publications; Munich, **2001**, pp. 296-328.
59. Zheng, Y., Miao, J., Maed, N., Frey, D., Linhardt, R. J. and Simmons, J. T. *J. Mater. Chem.* **2014**, *2*, 15029-15034.
60. Zheng, Y., Cai, C., Zhang, F., Monty, J., Linhardt, R. J. and Simmons, T. J. *Nanotechnology*, **2016**, *27*, 055102(8pp).
61. Xu, S., Zhang, J., He, A., Li, J., Zhang, H. and Han, C. C. *Polymer*, **2008**, *49*, 2911-2917.
62. Quan, S. L., Kang, S. G., Chin, I. J. *Cellulose*, **2010**, *17*, 223-230.
63. Miyauchi, M., Miao, J., Simmons, T. J., Lee, J. W., Doherty, T. V., Dordick, J. S. and Linhardt, R. J. *Biomacromolecules*, **2010**, *11*, 2440-2445.
64. Freire, M. G., Rita, R. A., Rute, A. T., Ferreira, S., Carlos, L. D., Jose, A. C., Silvac, L. D. and Coutinho, A. P. *Green Chem.* **2011**, *13*, 3173-3180.
65. Miyauchi, M., Miao, J., Simmons, T. J., Dordick, J. S. and Linhardt, R. J. *Sep. Tech.* **2011**, *2*, 1000110(4pp).
66. Hardelin, L., Thunberg, J., Perzon, E., Westman, G., Walkenstro, P. and Gatenholm, P. *J. Appl. Polym.* Sci. **2012**, *125*, 1901-1909.
67. Ahn, Y., Hu, D. H., Hong, J. H., Lee, S. H., Kim, H. J. and Kim, H. *Carbohyd. Polym.* **2012**, *89*, 340-345.
68. Hardelin, L., Perzon, E., Hagstrom, B., Walkenstrom, P. and Gatenholm, P. *J. Appl. Polym. Sci.* **2013**,*130*, 2303-2310.
69. Hou, L., Ranodhi, W. M., Udangawa, N., Pochiraju, A., Dong, W., Zheng, Y., Linhardt, R. J. and Simmons T. J. *ACS Biomater. Sci. & Eng*. **2016**, *2*, 1905-1913.
70. Liu, Y, Nguyen, A., Allen, A., Zoldan, J., Huang, Y. and Chen, J. Y. *Mater. Sci. & Eng. C.* **2017**, *74*, 485-492.
71. Mormann, W. and Wezstein, M., *Macromole. Biosci.* **2009**, *9*, 369-375.
72. Ostlund, A., Idstrom, A., Olsson, C., Larsson, P. T. and Nordstierna, L. *Cellulose*, **2013**, *20*, 1657-1667.
73. Lindman, B., Karlstrom, G. and Stigsson, L. *J. Mole. Liq.* **2010**, *156*, 76-81.
74. Liu, W. and Budtova, T. *Polymer*, **2012**, *53*, 5779-5787.
75. Remsing, R. C., Swatloski, R. P., Rogers, R. D. and Moyna, G. *Chem. Comm.* **2006**, *12*, 1271-1273.
76. Xu, A., Wang, J. and Wang, H. *Green Chem*. **2010**, *12*, 268-275.
77. Sun, N., Rahman, M., Qin, Y., Maxim, Y. L., Rodrıguez, H. and Rogers, R. D. *Green Chem.* 2009, *11*, 646-655.

78. Olsson, C. Cellulose Processing in Ionic Liquid Based Solvents, Ph.D. thesis, Chalmers University of Technology, Gothenburg, Sweden, June, 2014.
79. Olsson, C., Hedlund, A., Idstrom, A. and Westman, G. *J. Mater. Sci.* **2014**, *49*, 3423-3433.
80. Chae, D. W., et al., *Tex. Res. J.* **2002**, *72(4)*, 335-340.
81. Choe, E. W., Kim, S. N., *Macromolecules*, **1981**, *14(4)*, 920-924.
82. Fink, H. P., et al., *Progr. Polym. Sci*. **2001**, *26(9)*, 1473-1524
83. Kim, D. B., et al., *Tex. Res. J.* **2005**, *75(4)*, 331-341.
84. Wan, S. X., et al., *Polym. Adv. Tech.* **2009**, *20(11)*, 857-862.
85. Juza, J. *Czechoslovak J. Phys*. **1997**, *47*, 351-357.
86. Milas, M., Rinaudo, M., Knipper, M. and Schuppiser, J. L. Macromolecules, **1990**, *23*, 2506-2511.
87. Colby, R. H., Rubinstein, M. and Daoud, M. *J. Phys. II*. **1994**, *4*, 1299-1310.
88. Haas, D., Heinrich, S. and Greil, P. *J. Mater. Sci*. **2010**, *45*, 1299-1306.
89. Kuang, Q. L., Zhao, J. C., Niu, Y. H., Zhang, J. and Wang, Z. G. *J. Phys. Chem. B.* **2008**, *112*, 10234-10240.
90. Schuermann, J., Huber, T., LeCorre, D., Mortha, G., Sellier, M., Duchemin, B. and Staiger, M., *Cellulose* **2016**, *23*, 1043-1050.
91. Stubenrauch, C., Albouy, P. A., Klitzing, R. V. and Langevin, D. *Langmuir*, **2000**, *16*, 3206-3213.
92. Kim, M. W. and Cao, B. H. *EPL EuroPhys. Lett*. **1993**, *24*, 229-234.
93. Gu, S. Y., Wang, Z. M., Ren, J. and Zhang, C. Y. *Mater. Sci. & Eng. C*. **2009**, *29*, 1822-1828.
94. Demir, M. M., Yilgor, I., Yilgor, E. and Erman, B. *Polymer* **2002**, *43*, 3303-3309.
95. Bazbouz, M. B. An investigation of yarn spinning from electrospun nanofibres, Ph.D. Thesis, Heriot Watt University, Edinburgh, United Kingdom, May, 2009.
96. McKee, M. G., Wilkes, G. L., Colby, R. H. and Long, T. E. *Macromolecules*, **2004**, *37*, 1760-1767.
97. ILCO Chemikalien GmbH Germany, The Company for synthetic base fluids and additives, http://www.ilco-chemie.de/en/content/produkte/158-ionic-liquids/ (accessed January 22 2018).
98. Thiruvengadam, V. and Vitta, S. In Nanocellulose polymer nanocomposites fundamentals and applications; Thakur, V. K. Ed.; John Wiley & Sons, Inc., New Jersey, **2015**, Chapter 17, pp. 492-495.
99. Theron, S., Zussman, E. and Yarin, A. L. *Polymer*, **2004**, *45*, 2017-2030.
100. Yu, Y., et al., *Appl. Phys. A*. **2017**, *123*, 733-739.
101. Kumakura, M. *Polym. Adv. Tech*. **2001**, *12*, 415-421.
102. Liu, X. H., Pan, H. and Mazur, P. *J. Exp. Bio.* **2003**, *206*, 2221-2228.
103. Gottlieb, H. E., Kotlyar, V. and Nudelma A. *J. Org. Chem.* **1997**, *62*, 7512-7515.
104. Lovell, C. S., Walker, A., Damion, R. A., Radhi, A., Tanner, S. F., Budtova, T. and Ries M. E. *Biomacromolecules*, **2010**, *11*, 2927-2935.
105. Hall, C. A., Le, K. A., Rudaz, C., Radhi, A., Lovell, C. S., Damion, R. A., Budtova, T., Ries, M. E. *J. Phys. Chem. B.* **2012**, *116*, 12810-12818.

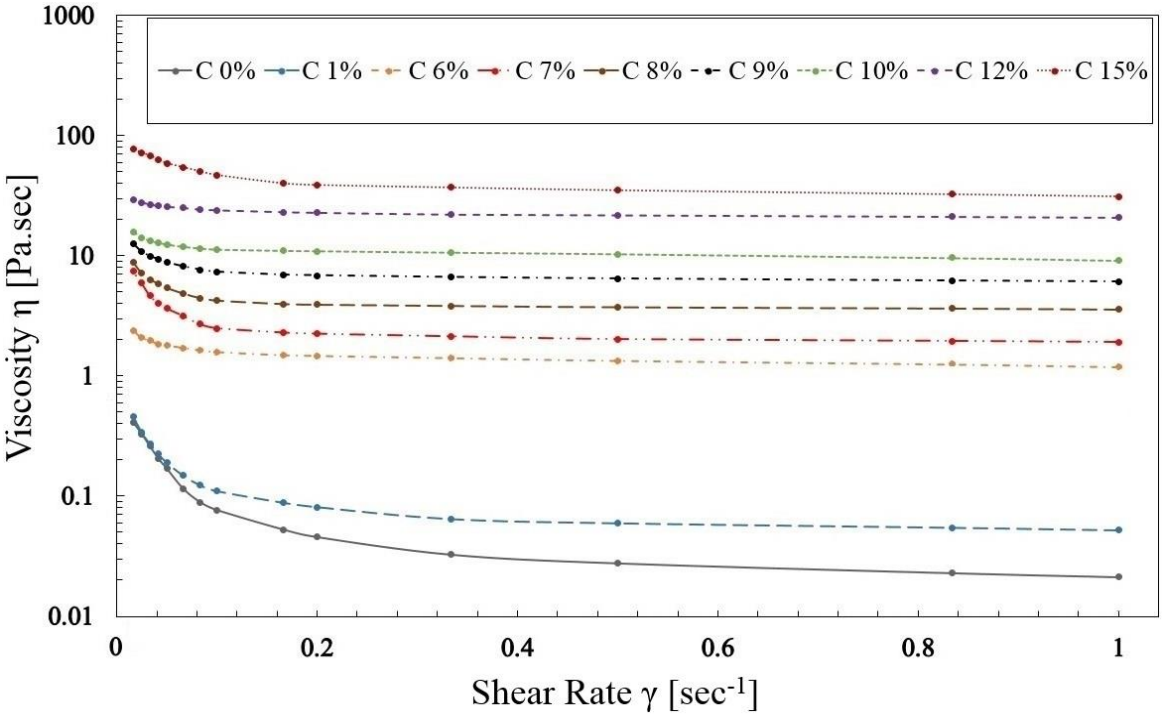

Figure 1. Changes of steady shear viscosity η, as functions of shear rate **γ**, for dissolving cellulose/([C2MIM][OAc]/MIM) solutions with different concentrations.

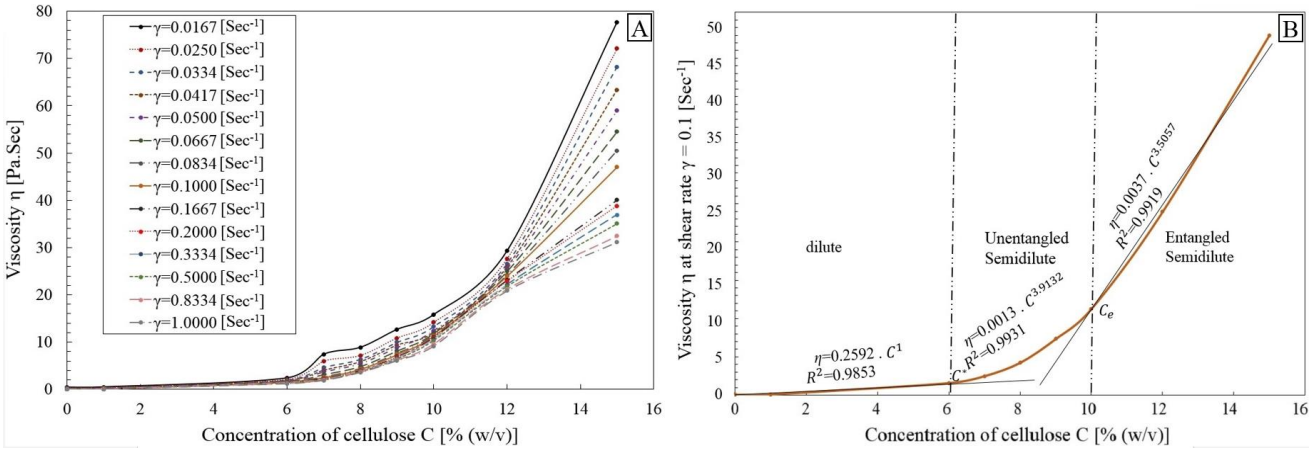

Figure 2. (A) Dependence of viscosity η at different shear rates γ on concentration of cellulose. (B) Dependence of viscosity η at shear rate γ of 0.1 [sec^{-1}] on concentration of cellulose.

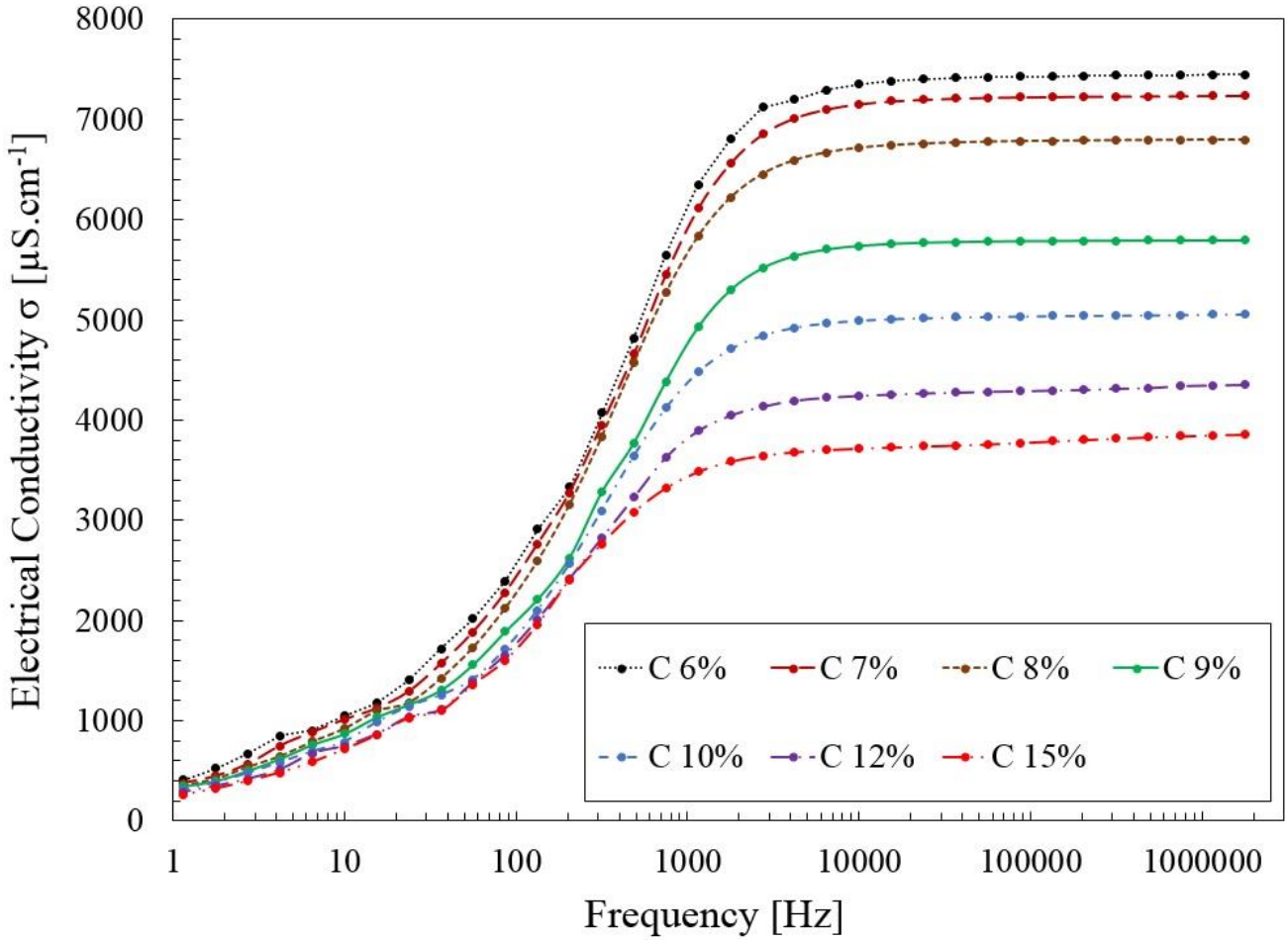

Figure 3. Electrical conductivity σ as function of frequency for dissolved cellulose in a binary of [C2MIM][OAc]/MIM (1:1 v/v) solutions at cellulose concentration of 6, 7, 8, 9, 10, 12, and 15% (w/v).

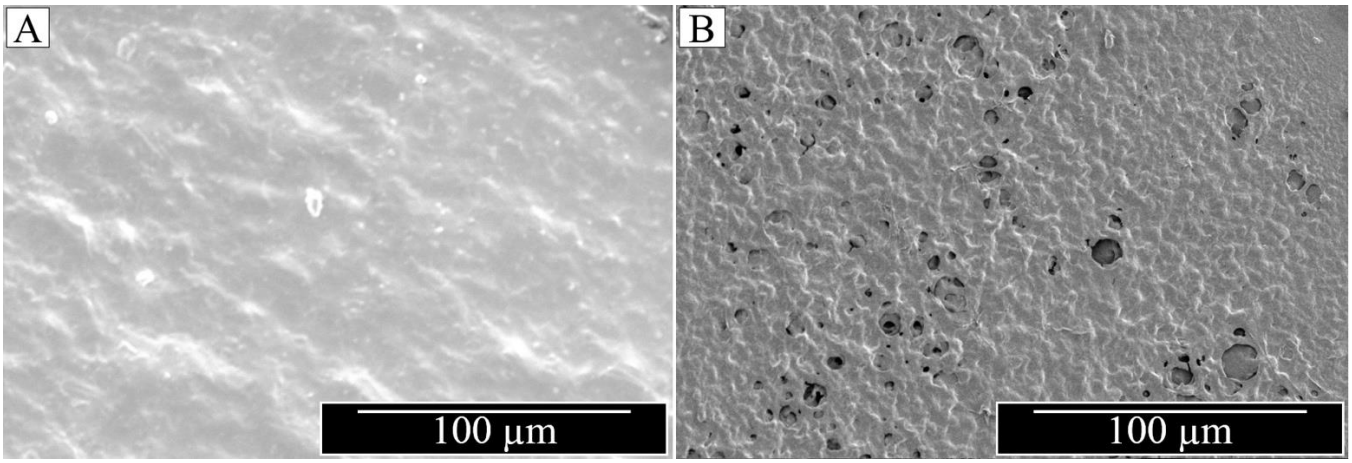

Figure 4. SEM images of electrospun cellulose/([C2MIM][OAc]/MIM) solutions at concentrations of (A) 6% w/v and (B) 10% w/v, when distilled water was used as a coagulation bath.

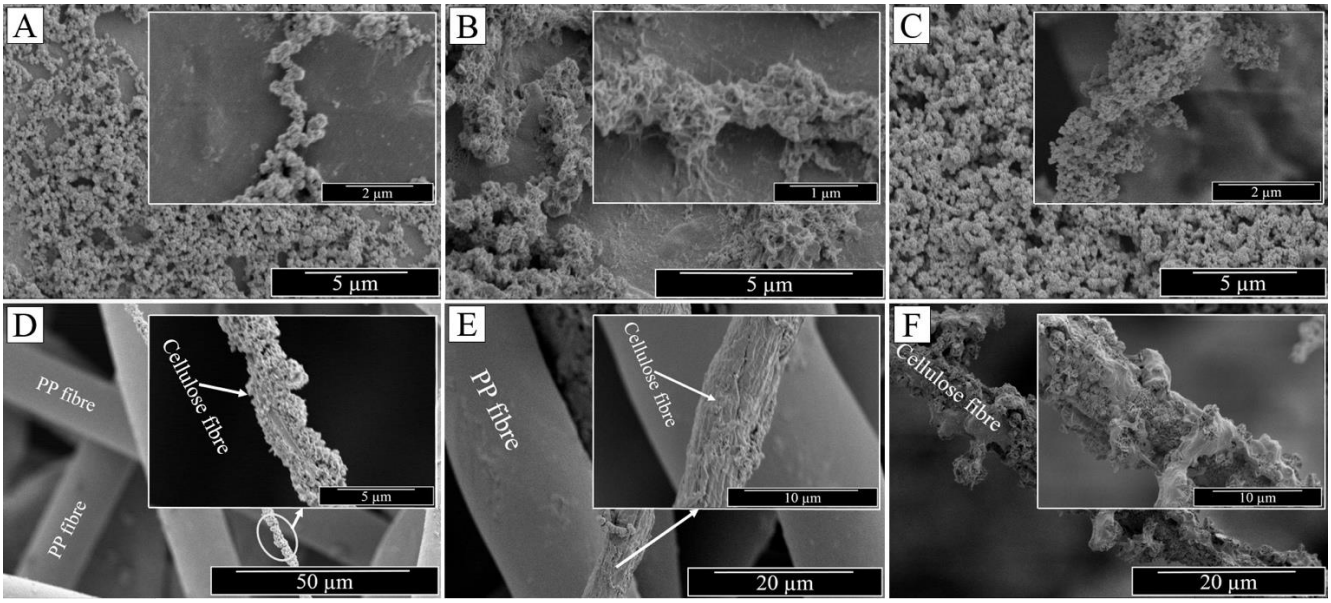

Figure 5. SEM images of electrospun fibres from cellulose/([C2MIM][OAc]/MIM) solutions at (A) 6% (w/v), (B) 8% (w/v), (C) 9% (w/v), (D) 10% (w/v), (E) 12% (w/v) and (F) 15% (w/v) cellulose concentration and directly immersed into distilled water bath at room temperature for 5 days after collection from ethanol coagulation bath.

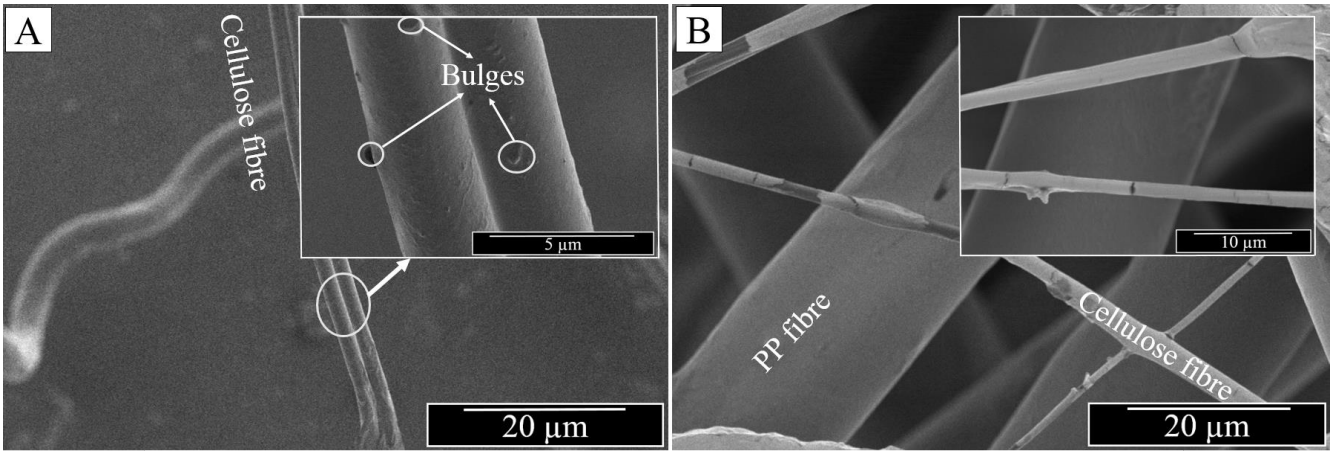

Figure 6. SEM images of the collected cellulose fibres at 10% w/v concentration from the ethanol coagulation bath after electrospinning course and directly were exposed to a liquid nitrogen (A) or were put into an oven at 70 ℃ for 24 h (B).

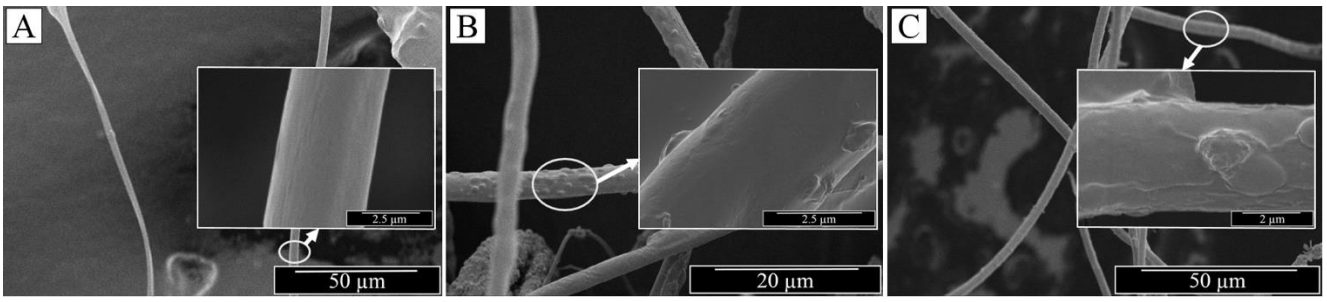

Figure 7. SEM images of the collected cellulose fibres at 10% w/v concentration from the ethanol coagulation bath after electrospinning course and directly were immersed in ethanol bath at room temperature for 1 day (A), 3 days (B) and 5 days (C).

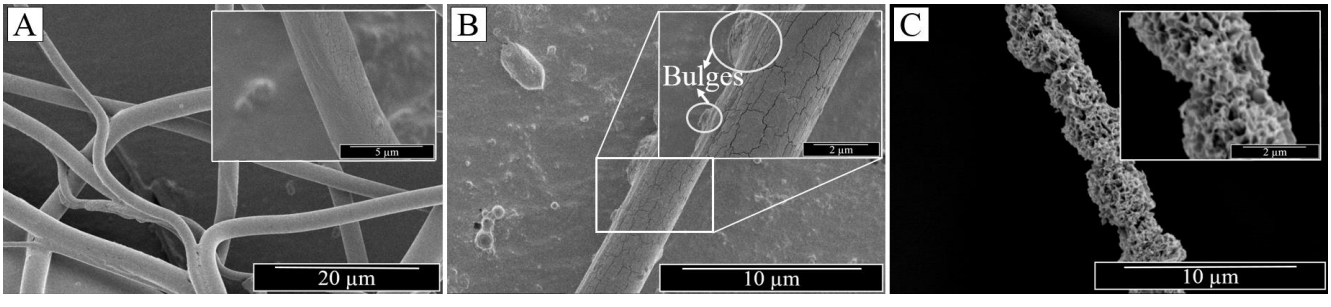

Figure 8. SEM images of the collected cellulose fibres at 10% w/v concentration from the ethanol coagulation bath after electrospinning course and directly were immersed in distilled water bath at room temperature for 1 day (A), 3 days (B) and 5 days (C).

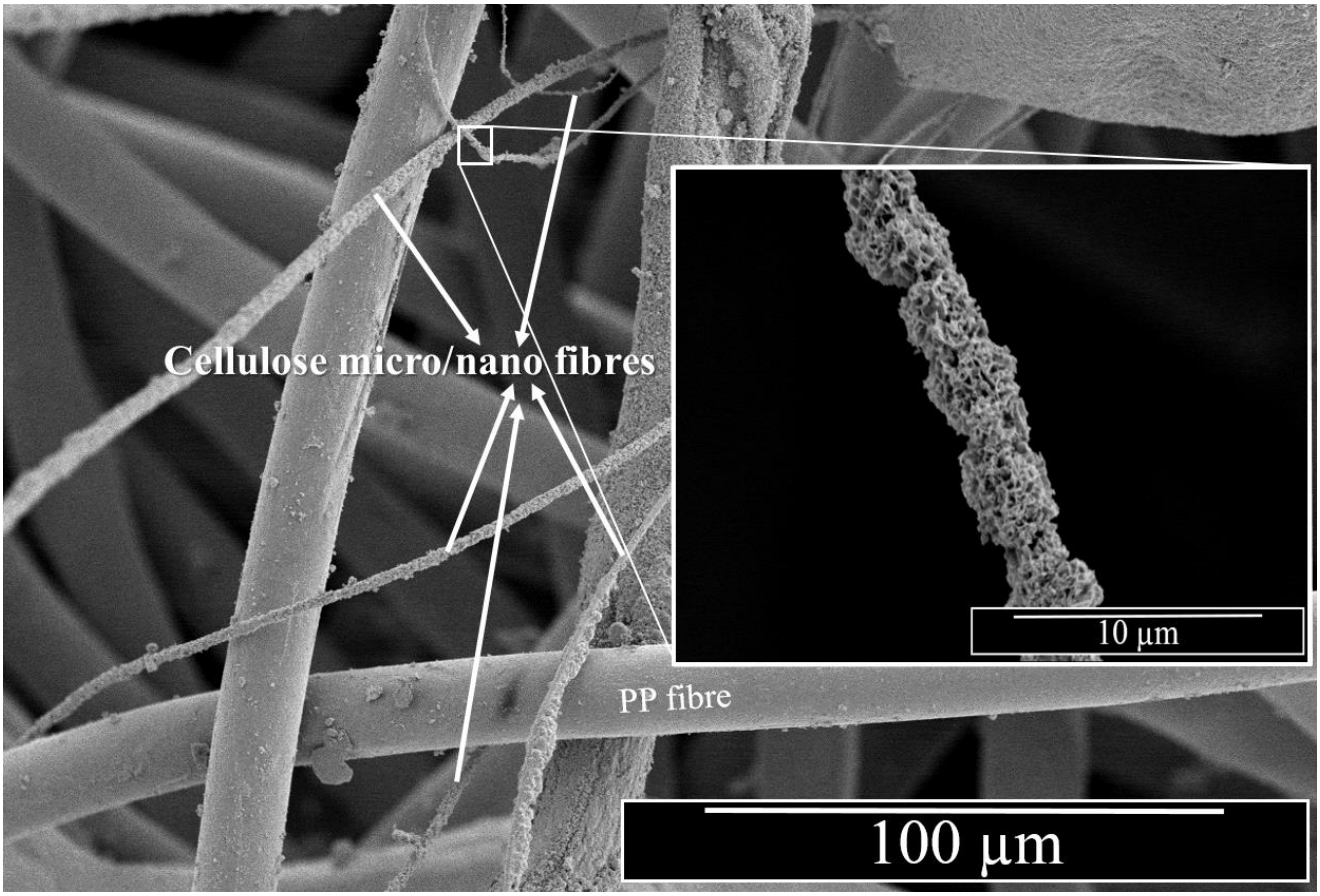

Figure 9. SEM image of the collected cellulose fibres at 10% w/v concentration from the ethanol coagulation bath after electrospinning course and were immersed in distilled water bath at room temperature for 5 days. Electrospun cellulose fibres are showing a macroporous structure on their surfaces, due to the larger [C2MIM][OAc] extraction during the 5 days immersion in distilled water.

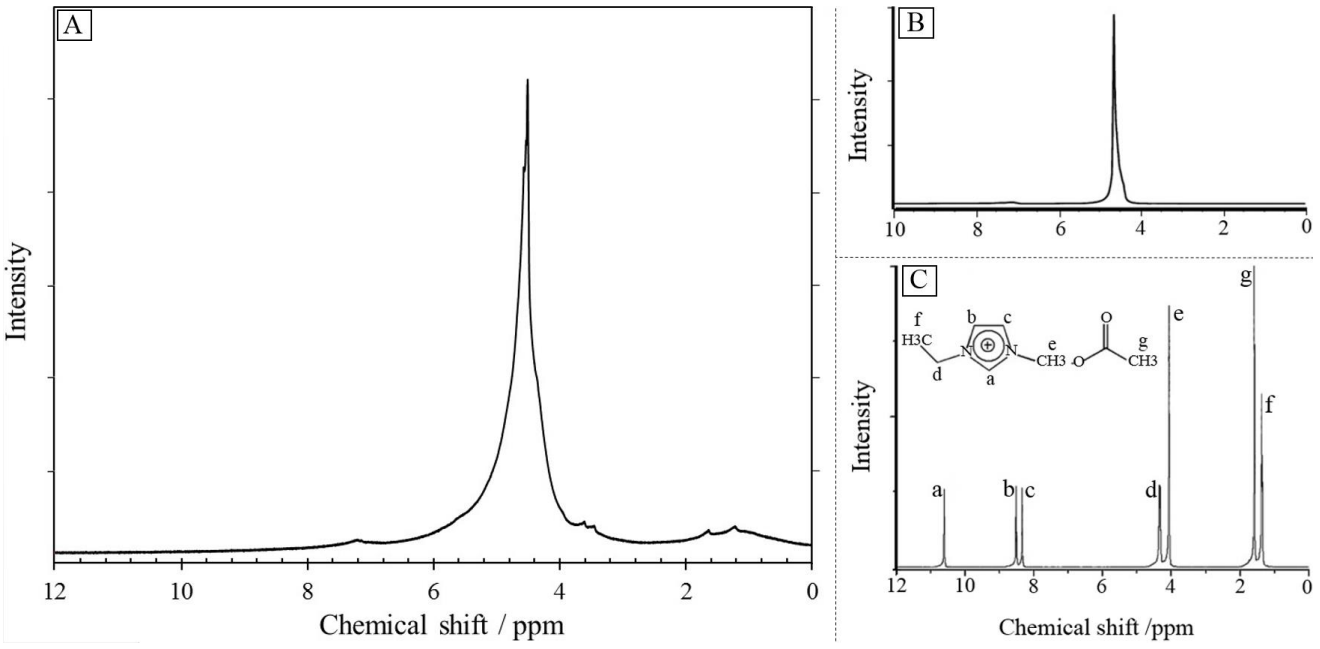

Figure 10. (A) ^{1}H NMR spectrum of the collected electrospun cellulose fibres from the ethanol coagulation bath after electrospinning and directly were immersed in deuterium oxide (D2O) at room temperature of 23 ±2 ℃ for 5 days, (B) ^{1}H NMR spectrum of (D2O) with one OH proton peak at a chemical shift of approximately 4.8 ppm which contributed to the residual H2O[102, 103], (C) ^{1}H NMR spectrum of pure [C2MIM][OAc] obtained at 20 °C[104]. The inset shows the chemical structure of 1-ethyl- 3-methyl-imidazolium acetate [C2MIM][OAc].

Table I. The electrospinning of nanofibres from native cellulose dissolved in different types of ionic liquids (ILs) and co-solvents.

Cellulose name	Ionic liquid – with or without Co-solvent	Pre- treatment of cellulose (H,T)	Dissolving of Cellulose (C, H,T)	Collecting of nanofibres (M,H)	ES Environmental parameters	ES Electric field	ES Distance
Pulp with DP of 1000 and Mw of 5800000.	[C4MIM][Cl]	----------	10 wt.% Cellulose/[C4MIM] [Cl],70°C, Micro-wave 4-5 sec.	Coagulation bath / Ethanol.	----------	15 - 20 kV- DC	15 cm
Cotton linters with DP of 1600.	[AMIM][Cl], [AMIM][Cl]/DMSO (1;1,1;2,1;4,1;8)w/w.	70 °C for 3 h in a vacuum oven.	1, 3, 5 wt. % Cellulose in [AMIM][Cl] or [AMIM][Cl] /DMSO 80 °C, 2 h.	Parallel copper wires rotating drum, AL foil ethanol bath.	Constant relative humidity of 60 %.	15 KV-DC	12 cm
Cellulose powder with Mw of 19400.	[C4MIM][Cl] (solid) heated 80 °C, in an Oil Bath. [C4MIM] [Cl] /DMSO	----------	(1.5, 2.4, 3, 4, 5) wt. % Cellulose in [C4MIM][Cl] /DMSO, 80 °C, 30 min.	Water bath, then the NW mat was dipped in water at 70 °C for 30 min.	Spinneret was set at 100 °C by using an external circulator.	15 KV-DC	15 cm
Cellionic (5% cellulose DP of 1100 in [C2MIM][OAc]) with 1.2 - 7 wt. % MWCNTs.	[C2MIM][OAc]	----------	(1.5-5) wt. % cellulose in [C2MIM][OAc] as a shell and cellulose + MWCNTs + [C2MIM][OAc] as core.	Water / ethanol mixture bath.	----------	18 - 22 KV-DC	9 cm
Raw cellulose fibres with Mw of 53000.	[C2MIM][OAc]+ [C10MIM][Cl]	Dried in oven at 105 °C for 12 h.	8 wt. % Cellulose in [C2MIM][OAc] + [C10MIM] [Cl]) (1:1) w/w.	Water bath, then the NW mat in water/ethanol.	----------	20 kV-DC	12 cm
Cellionic (5% cellulose DP of 1100 in [C2MIM][OAc] + 1.75 % Cellulose in [C2MIM][OAc].	[C2MIM][OAc], 80°C	----------	Cellionic (5% cellulose (DP1100) in [C2MIM][OAc] + 1.75 wt. % Cellulose in [C2MIM][OAc].	Al (20 µm thick) was grounded and placed on the bottom of water coagulation bath.	----------	18 - 19 KV- DC	9 cm
Cellulose pulp DP of 750.	[C2MIM][OAc] + (DMF, DMAc, DMSO) (10-90 %).	Pulp were cut into 1mm pieces, then dried in an oven at 80 °C for 12 h.	2.5 wt. % Cellulose pulp / ([C2MIM][OAc] +DMSO or DMF or DMAc) mixture was stirred at 80°C & 12 h.	A rotating collector (10 cm) (25 rpm) covered with an AL sheet was partly dipped in water bath.	Constant relative humidity 60 % and temperature of 20 °C.	10 - 50 KV- DC	10 cm
Cellulose powder.	[C2MIM][OAc] + (DMF, DMAc) (2:1, 1.5:1, 1:1) w/w.	----------	(6.3, 7.2, 8.3) wt. % cellulose with ([C2MIM][OAc] + (DMF or DMAc)).	A rotating wired cylinder type collector. Then the mat was immersed in Ethanol bath (4 °C, 2 hour) then dried (50 °C, 24 hour).	----------	30 KV-DC	15 cm
Dissolving pulp with viscosity 500 - 900 mL/g, and a DP of 620 -1360.	[C2MIM][OAc] + DMSO (1 :1)w/w.	Pulp was disintegrated (SCAN -C18: 6) dried (80°C, 12 h)	(5, 7.5, 10, 12.5) wt.% Cellulose in [C2MIM][OAc] + DMSO (1 :1) w/w.	Rotating collector 25 rpm (10 cm) covered by AL foil which was partly submerged in a water bath.	Constant relative humidity of 65 % and temperature of 20 °C.	10 - 50 KV- DC	10 cm
Cellulose pulp with DP of 1100.	[C2MIM][OAc]	----------	1.55 wt. % Cellulose pulp / [C2MIM][OAc] mixture was stirred in oil bath at 80 °C for 8 h.	3 mg / mL Mg (OH) 2 NPs in deionized water as coagulation bath.	----------	15 - 20 KV- DC	10 cm
Natural Cotton balls.	[C2MIM][OAc]	----------	1.2wt. % cotton solution in [C2MIM] [OAc] at 80°C for 8 h.	de-ionized aqueous coagulation bath	----------	15 - 20 KV- DC	10 cm
Cellulose pulp DP of 1100.	[C2MIM][OAc]	----------	1.5 wt. % Cellulose pulp / [C2MIM][OAc] mixture was stirred at 80 °C. Cellulose/heparin blended shell and Fe_3O_4 heparin as a core were also prepared.	distilled water coagulation bath - water/ethanol mixture coagulation bath	Temperature of 20 ± 3 °C with relative humidity of 30 ± 5%.	12 - 18 KV- DC	15- 20 cm
Pine Kraft pulp with 87% alpha cellulose.	[C4MIM][Cl] (solid) was heated to 80 °C in a water bath until melted.	----------	2 and 3 wt. % Cellulose in [C4MIM][Cl] at 1 h mixing and 90 °C with loading of Ibuprofen.	water bath collector	The heating cover temperature was set to 103 °C.	10 KV-DC	12 cm

Abbreviations: ES: Electrospinning, M: Material, H: Temperature, T: Time, C: Concentration, AL: Aluminium, SEM: Scanning Electron Microscope, VIS: Viscosity, ST: Surface Tension, EC: Electrical Conductivity, TS: Tensile Strength, RH: Relative Humidity, AT: Adsorption Test, SEC: Size Exclusion Chromatography, ATR-FTIR: Attenuated Total Reflectance Fourier Transform Infrared, XPS: X-ray Photoelectron Spectroscopy, FE-SEM: Field Emission Scanning Electron Microscope, AAS: Atomic Absorption Spectroscopy, LC: Liquid Chromatography, MS: Mass Spectrometry, TGA: Thermogravimetric Analysis, DTG: derivative thermal gravity, FT-IR: Fourier transform infrared spectroscopy, TT: Tribological Testing, CAT: Contact Angles Testing, CCA: Cell Cytotoxicity Assay, DRA: Drug Release Assay, DMAc: Dimethylacetamide, DMF: Dimethyl formamide, DMSO: Dimethyl sulfoxide, MIM: 1-Methylimidazole, [C2MIM][OAc]: 1-Ethyl-3-methylimidazolium acetate, [C4MIM][Cl]: 1-Butyl-3-Methylimidazolium Chloride, [AMIM][Cl]: 1-allyl-3-methylimidazolium chloride, [C10MIM][Cl]: 1-decyl-3-methylimidazolium chloride.

Table II. Surface tension of [C2MIM][OAc], MIM and solutions of cellulose/([C2MIM][OAc]/MIM) (1/1: v/v) at room temperature of 23±2°C.

Type of solution	[C2MIM][OAc]	MIM	[C2MIM][OAc]/ MIM (1/1:v/v)	C 6% w/v	C 7% w/v	C 8% w/v	C 9% w/v	C 10% w/v	C 12% w/v	C 15% w/v
Surface tension ± SD [$mN.m^{-1}$]	45.78 ± 0.76	34.3 ± 0.55	41.82 ± 1.12	40.48 ± 0.32	39.87 ± 0.42	39.21 ± 0.53	38.88 ± 0.52	38.26 ± 0.78	37.67 ± 0.85	37.19 ± 0.91